Laser-Wakefield Electron Accelerators

Adam A. S. Green

May 10, 2015

Abstract

In the late 1970's, Tajima and Dawson published a seminal paper in *Physical Review Letters* outlining a new kind of electron accelerator that was orders of magnitude smaller than conventional accelerators. They showed that by leveraging the high energy gradients of laser-excited plasmas, electrons could be accelerated over centimeter length scales to energies upwards of 10×10^9 eV. Their proposal was untenable at the time, as it required lasers with peak intensities far beyond the technology of the era. It has only been recently, through a combination of modern laser technology and powerful new numerical methods, that researchers have been able to make dramatic progress in the field. Now, several groups are poised to deliver on the original promise of Tajima and Dawson.

In this work, we review the field of Laser Wakefield Electron Accelerators (LWPA) covering the historical beginnings, the physical underpinnings, and closing with a discussion on current state-of-the-art experimental results.

Contents

1 Introduction

Conventional methods of electron acceleration use an TM-mode rf field propogating in a waveguide to provide the acceleration gradient. Because the electric field in a TM-mode is parallel to the propogation axis, electrons injected with the right velocity can co-propogate with and be accelerated by the electric field gradient. However, waveguide field gradients are fundamentally limited by electric breakdown on the walls of the

waveguide to around 1×10^6 eV m^{-1}[], which means to achieve the 50 GeV energies currently used at the Stanford Linear Accelerator Center (SLAC), the waveguide has to be about 2 miles long. In contrast, the acceleration gradients in plasmas can easily exceed 10 GeV m^{-1}, thereby allowing electrons to be accelerated over centimeters for similiar energy gains.[] The study of LWPA is strongly motivated by this promise of table-top electron accelerators.

The broadest application of high-energy electrons is for their use in free-electron x-ray lasers: the development of which has allowed investigation of structures in biology, solid state physics, as well as pioneering techniques in medical imaging.[15] Currently, free-electron x-ray lasers are tied to the linacs that provide them with high-energy electrons. These linacs consume large amounts of real-esate and are expensive to maintain, with large overhead for maintence and personal. Not only does this prevent the disemmination of x-ray lasers in the broader scientific community, but also in the unlikely event that it is damaged or its funding is cut[1], there wouldn't be many alternatives for a tool that is indespendible for many areas of modern science.

[1] The famous cancellation of the Superconducting Super Collider in Texas due to budget problems in one dramatic example

LWPA offer an option that is compact and inexpensive by comparison. Although LWPA will never supplant linac's[2] they offer a complimentary approach at a fraction of the cost and real-estate. Much like the impact of personal computers introduced in the era of massive supercomputers, the impact of a small cheap x-ray laser, while difficult to gauge, will definitely be dramatic.

[2] This is because the beam produced by LWPA is not continuous; the nature of LWPA technology means that the electrons beam produced will be an intense bunch, rather than a continuous beam like SLAC.

The quest to produce high-energy electrons has four main goals: getting high-energy electrons; having a narrow energy distribution; producing collimated beams; and hav-

ing a large number of electrons produced.

In the context of free-electron lasers, these are important for the following simple reasons: the frequency of the x-rays scales with the square of the energy of the electrons: the higher the energy, the smaller the length scales we can probe; the narrower the electron energy distribution, the narrower the x-ray linewidth; and the beam quality (number of electrons and angular spread) will also directly effect the x-ray laser coherence.[] Over the years there have been many different proposals to implement LWPA, but it was only within the past decade that LWPA technology was capable of meeting the above requirements. In the following section, we will briefly review the historical development of LWPA.

1.1 History

Tajima and Dawson originally proposed shooting a high-intensity laser pulse at a plasma[17]. The photon-pressure of the laser would generate a wakefield very similar to a boat moving through water and electrons could be accelerated by this wakefield. Unfortunately, the lasers of the day were unable to get to the high intensities required and it was only the invention of chirped-pulse amplification (CPA) fifteen years later that allowed serious progress in the LWPA field to occur[1]. Even once this issue had been overcome there were still severe experimental constaints involved, as exciting the plasma wave requires the laser to be at the resonant frequency of the plasma, ω_p, which scales with the square-root of the plasma density. For typical laboratory plasmas, this resonant frequency was out of reach for the lasers of the time. To overcome this problem several

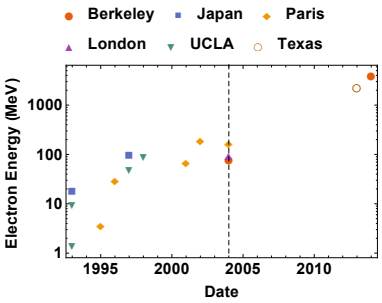

Figure 1: The progress of laser plasma wakefield acceleration by the total energy of the electrons. The dashed line shows the advent of quasi-monoenergetic electrons, until that point the electron bunches had large thermal tails. *This data was gathered from the web of science abstract list*

LWPA schemes were devised; the two major ones being the plasma beatwave accelerator and the self-modulated laser accelerator. Although the mechanics of these schemes differed the underlying principle was to excite the plasma with a beatwave generated by spatio-temporally overlapping two lasers detuned from each other by $2\pi\omega_p$. This effort was moderately successful: in 1995 electrons were successfully accelerated to energies in excess of 40 MeV[]. Unfortunately, these electron beams had large Maxwellian energy distributions, making them untenable for practical applications which require mono-energetic electrons.

A breakthrough occured in 2002, when using advanced numerical methods Pushkin predicted the bubble regime, whose properties would solve many of the problems historically faced by LPWA schemes[]. The bubble regime is so named as it used a laser powerful enough to completely expel electrons from the pulse region, creating a ion 'bubble'. One of the most attractive properties of the bubble regime was its predicted ability to produce mono-energetic electrons.

In 2004 this approach bore fruit, as three papers published simultaneously in Nature[14, 7, 8], demonstrated quasi-monoenergetic electron bunches in the bubble regime. Their results were soon extended to achieve energies of 1 GeV in 2006 [13].

In 2013, a group at UT Austin produced a collimated, quasi-monoenergetic electron beam at 2.3 GeV[19], and in 2014 the Esarey group at UC Berkeley produced a 4 GeV[12] beam. These recent developments bring the field within striking distance of the LCLS free electron laser at SLAC, which uses electrons accelerated to 17.4 GeV[].

In the following section, we will discuss the physics of Laser-Plasma-Acceleration, and

then discuss the two most recent experiments from UT Texas and UC Berkeley.

2 The Physics of Laser-Plasma-Acceleration

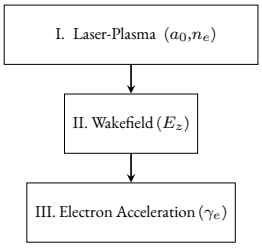

Figure 2: The LWFA process.

The LPWA process is divided into three main topics, as shown in Figure 2. First the intense laser, characterized by the normalized field strength $a_0 = e\mathrm{A}/m_e c^2$, with A as the vector potential, interacts with the plasma, characterized by the plasma density n_e. This produces a longitudinal density modulation, which in turn gives rise to a longitudinal electric wakefield, E_z. The wakefield then accelerates injected electrons to a relativistic energy γ_e. In this section, we review these three related phenomena: the creation and evolution of a plasma wakefield; the dynamics of electron acceleration; and the propogation of intense laser pulses in plasmas[3].

[3] Due to the complicated nature of the theory of LPWA in 3D relativistic fields, we will mainly discuss these topics in the linear regime and show the numerical results of their extension into the 3D relativistic regime.

2.1 The Interaction of Lasers and Plasmas and Creation of Wakefields

The mass of the ions in the plasma is many orders of magnitude larger than the electrons, so it is valid to approximate the behaviour of the plasma as a fluid of mobile electrons against a static background of ions. The motion of the electrons is then governed by the combination of the Lorentz force law, the continuity equation, and Poisson's equation. Additionally, if the intensity of the laser is small enough, then these equations can be linearized and are referred to the cold-fluid equations[10]. In the cold-fluid

regime, the Lorentz force takes the following form:

$$\frac{\partial \mathrm{p}}{\partial t} + (\mathrm{v} \cdot \boldsymbol{\nabla})\mathrm{p} = e\left(\boldsymbol{\nabla}\Phi + \frac{\partial \mathrm{A}}{\partial t} - \mathrm{v} \times \boldsymbol{\nabla} \times \mathrm{A}\right) \tag{1}$$

Where p, v are the electron's momentum and velocity, and Φ and A are the scalar and vector potentials of the total field.

The linear behaviour of this fluid will be dominated by the force of the electric field on the electrons, accelerating them in the polarization plane. This is called the 'quiver' momentum[4].

[4] So named because the electron will undergo rapid oscillations while its time averaged acceleration will be zero, so it will appear to be quivering

Considering the next leading order behaviour of the electron momentum and averaging over one optical cycle, we get a force that is proportional to the intensity gradient of the laser pulse. This is known as the ponderomotive force[] and can be thought of as the radiation pressure of the laser pulse, acting to push electrons away from the local space of the laser pulse. As the laser propogates through the plasma, the ponderomotive force will drive a density wave known as a plasmon, analogous to the physical situation of shooting a cannonball underwater.

This can be seen as the solution for the density flucations in the cold-fluid regime is the wave equation[]:

$$\left(\frac{\partial^2}{\partial t^2} + \omega_p^2\right)\delta_{n_e} = c^2\nabla^2\frac{a^2}{2} \tag{2}$$

where a is the normalized vector potential and δ_{n_e} is the density flucuation of the elec-

tron fluid, with the resonant frequency of the electron fluid given by:

$$\omega_p = \sqrt{\frac{e^2 n_e}{m_e \epsilon_0}}, \tag{3}$$

Where m_e, n_e, and e are the mass, density and charge of the electron, respectively.

We can connect the variations in density to the electric field produced using Possion's equation, where under the assumption of periodic behaviour in E, reduces to:

$$\mathrm{k} \cdot \mathrm{E} = \frac{\delta n_e}{\epsilon_0} \tag{4}$$

Showing that an electric field oriented along the propogation axis will co-propagate with density wave, oscillating π out of phase. This is shown in the linear and non-linear 1D regime in Figure 3a. This field E_z is refered to as the wakefield[] and will be used to accelerate the injected electrons. As in the rf linear accelerator, the only way to accelerate electrons is by creating a propogating wave whose electric field points along the propogation axis.

As all modern LWPA approaches operate in the bubble regime we have to further extend our simple 1D model to a highly non-linear 2D or 3D model. We can access this regime by eliminating the assumption that $a \ll 1$ and an analytic solution in 1D can still be found[]. However, in 2D or 3D, the equations become intractable and numerical simulation is required. An example of a numerical solution in a non-linear 2D model is shown in Figure 3b.

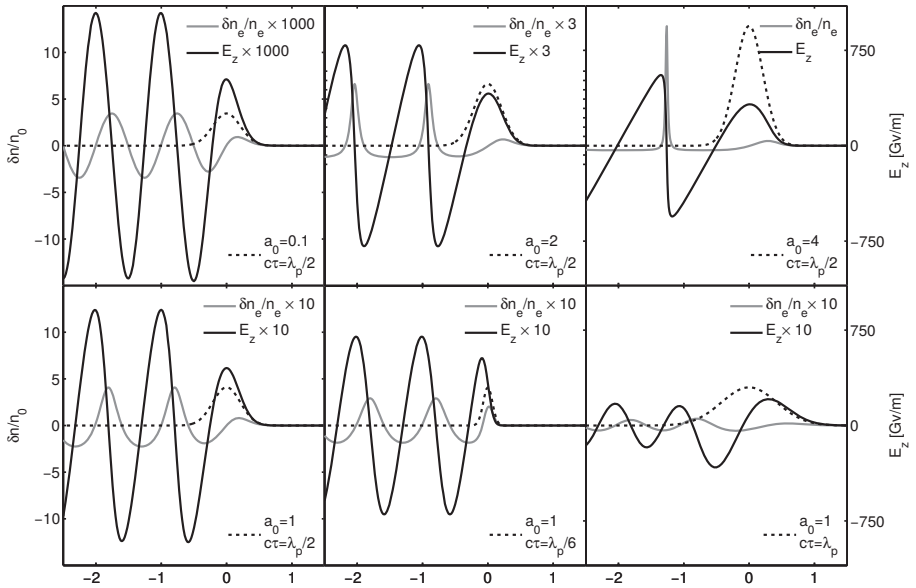

(a) Showing plasmons generated with varying strengths of the peak amplitude of the laser pulse.[9] The laser pulse is the dashed line, the density perturbation is the grey line, and the longitudinal electric field E_z is the black curve. The x-axis is showing the normalized co-ordinate $\zeta = kz - wt$, which shows the evolution of the phase-front. Different scenarios are shown: from left to right, the normalized field strength variable ($a = eA/m_e c^2$) is varied, and from top to bottom, the duration of the laser pulse is changed. *Figure courtesy of Guillaume Genoud, Lund University*

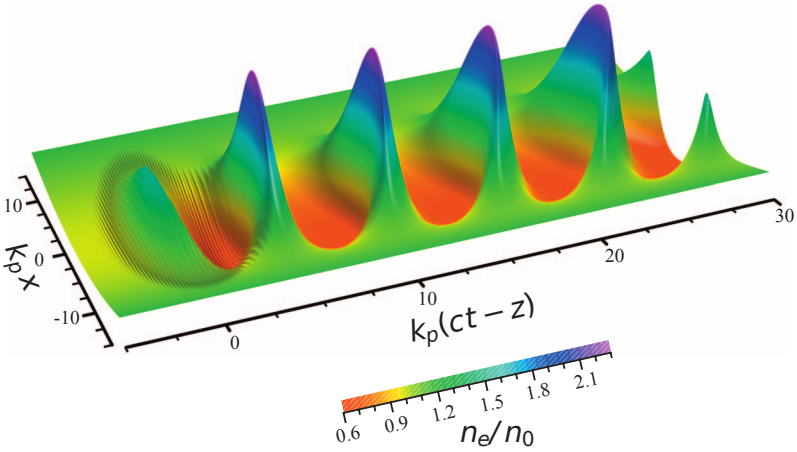

(b) Numerical simulation for a 2D, non-linear model. Many of the features in the 1D model remain– the signature 'leaning' of the density pulse as it becomes non-linear being the most striking.

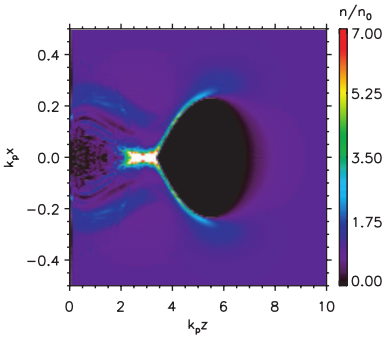

Figure 4: An example of the bubble regime created by a laser pulse with $a = .3$. The laser is moving toward the right, and $\delta_n = \frac{n}{n_0}$, with n being the density of the electrons and n_0 being the density of the ions. The coordinates are dimensionaless and show the evolution of the phase-front.[5]

An example of the bubble regime is shown in Figure 4

2.2 Electron Dynamics

Now that we have discussed the wakefield, we can discuss the actual dynamics of electron acceleration. This is divided into two topics: electron trapping, and electron acceleration.

2.2.1 Trapping Electrons

Previously, we have mentioned that electrons need to be injected into the wakefield. This is because the wakefield will be co-propogating with laser pulse– moving close to the speed of light, a stationary electron in the lab frame won't have enough interaction time to be accelerated. Some minimum electron velocity is required, and this can either be achieved by externally injecting electrons, or by taking advantage of the non-linear processes in the bubble regime to self-inject electrons from the surrounding fluid[5]. To illustrate the point, several phase-space trajectories of test electrons with various initial momenta are shown in Figure 5. Self-injection is currently favoured by experimentalists as the alternative, external injection, requires electrons that have already been accelerated to high energies. Self-injection makes use of the electrons in the fluid, allowing the acceleration process to be self-contained.

Althought the equations governing the self-injection process in the bubble regime are highly non-linear, we can give a broad strokes explanation of its dynamics by thinking

[5] Interesting, although self-injection happens in non-linear fields in both 1D and 3D, it occurs by different physical processes[6]. We will be focusing on the 3D case in this review.

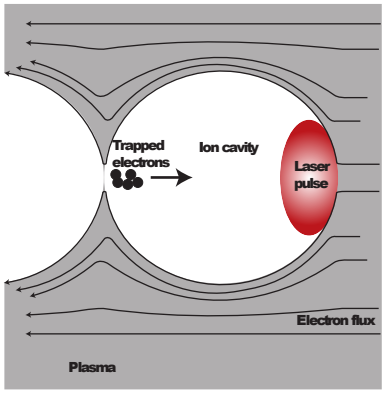

Figure 6: A schematic of the bubble regime.[9]

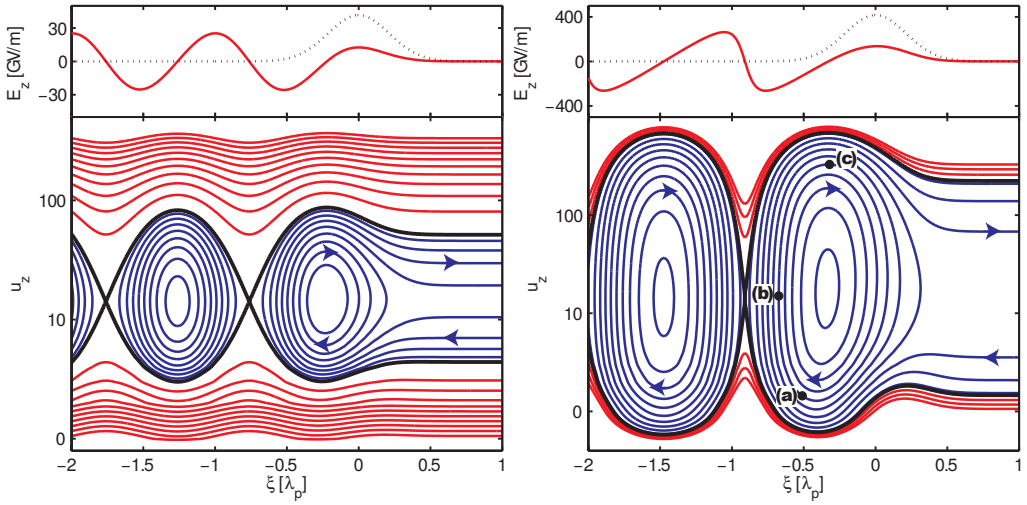

Figure 5: The various trajectories of electrons at different initial normalized momentum ($u_z = p/m_e c^2$) in the reference frame of the laser pulse, which is moving at an relativistic energy $\gamma = 13$ in the lab frame. An electron injected at the phase-space point a will be trapped, and accelerated by the wakefield through point c until it gains its maximum momentum at point c. At point c, it will be 'dephased' as it has overtaken the accelerating wakefield, at which point it drops back to point a. An experiment has to be designed so that the electrons are harvested at the dephasing point c. The black curve is the seprratric, which seperates trapped electrons from untrapped electrons. ζ is the normalized co-ordinate showing the phase-front evolution.

of the bubble as an ion-cavity moving relativistically through an electron fluid. As the bubble propogates, a small sheath of electrons will form a boundary layer between the ion-cavity and the surrounding electron fluid. This sheath will be in contact with the relativistic fields of the cavity for the longest time, and is the best candidate to be accelerated. Much like a comet's trajectory can be altered by the Sun's gravitional potential well, the ion-cavity can deflect electrons as they move past, an example of this is shown in Figure ??. If the bubble's radius changes on timescales much faster than the electron's motion, then a trajectory that previously would only have been altered is now within the 'event-horizon' of the bubble, and can be trapped. In fact, the bubble's radius will

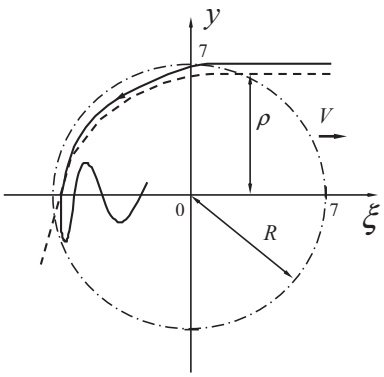

Figure 7: Showing a trapped, and untrapped trajectory of an electron. The bubble parameters are $R = 7, \gamma_0 = 4$

change. The ponderomotive force not only will push electrons along the propogation axis, it will additionally push electrons in the radial direction. This means that the front of the laser pulse will be propogating through a less dense region and will diffract and exand, in turn expanding the bubble. There are strict requirements on the radius of the bubble for this to occur, which additionally imposes experimental constraints on the waist of the laser pulse. Through use of a combination of numerical and analytical analysis the specific requirement for the radius of the bubble for self-injection to occur is given by: $R/\sqrt{2} > \omega_0/\omega_p$, where R is the radius of the bubble, and ω_0 is the laser frequency.[11]. An example of this trapping dynamics is shown in Figure ??

Now that we have shown how electrons are injected into the wakefield, we can discuss the dynamics of their acceleration.

2.3 Electron Acceleration

The plasma bubble will set up a very high GeV cm^{-1} acceleration field, but the limiting factor in the total energy gain is the distance the electrons are accelerated for. We have already alluded to the dephasing length in Figure ??, where the electron outruns the wakefield. However, there are two additional length scales that have to be considered.

The first, $L_{\text{PulseDepletion}}$, occurs because the interaction with of the laser-plasma will dissipate the energy of the initial laser pulse. The energy in the initial laser will be transfered to the plasma wake where it will ultimately be dissipated as heat. In 1D, this can be approximated quite well by simply equating the total energy of the laser to the energy in the wakefield: $E_z^2 L_{pd} = E_L^2 L$, where E_z is the wakefield and $E_L,\ L$ refer to the laser

field and pulse length, respectively[5].

In a non-linear 3D regime, an estimate based on the 1D non-linear was found to still be accurate. There the pulse depletion is given as the laser-front is etched away as it excites the wakefield. This etching velocity is a result of the ponderomotive diffraction occuring, and requires and time scale of ω_p^{-1} to build up. The velocity is given as $v_{\text{etch}} \approx c\omega_p^2/w_0^2$ [4]. The pump depletion length is then given by:

$$L_{\text{etch}} \approx \frac{c}{v_{\text{etch}} c\tau_{\text{FWHM}}} \tag{5}$$

The second, $L_{\text{Diffraction}}$ is the most important, as it is the limiting length scale for all modern experiments. This length scale is due to the inherent diffraction of lasers. In order to achieve the intense energies necessary for the bubble regime and to meet the requirements on the bubble radius, the lasers need to be focused down to a specific spot size. As soon as the minimum spot size is reached the laser will begin to diffract. The length scale over which the laser is approximately the spot size is the Rayleigh length.

As we have already discussed, the final length, $L_{\text{Dephasing}}$ is analogous to what happens when a surfer outruns the wave they are on; no longer being accelerated, they slow down as their energy is dissipated to the wave. Similarly, electrons can outrun the plasma bubble. In 1D, this concept can be simply defined as the length it takes for the electron's phase to slip by one-half of the plasmon. For the 3D theory theory in the bubble regime, a good approximation of this can be found by estimating the electron's velocity as c, and asking when it will overtake the bubble, which is moving at a slower

Model	L_d	L_{pd}	L_{diff}
Linear	$\frac{\lambda_d \omega_0^2}{\omega_p^2}$	$\frac{c\omega_0^2\tau}{\omega_p^2 a_0^2}$	$\frac{\pi\lambda_p^2}{\lambda_0}$
Non-Linear	$\frac{4}{3}\frac{c\omega_0^2}{\omega_p^2}\sqrt{a_0}$	$\frac{c\omega_0^2\tau}{\omega_p^2}$	$\pi\frac{a_0\lambda_p^2}{\lambda_0}$

Table 1: The scaling laws for limiting lengths in LPWA.

velocity $v_\phi - v_{\text{etch}}$. Solving this gives

$$L_d \approx \frac{c}{c - v_\phi} R \tag{6}$$

where R is the bubble radius. In Figure 8, we can see the length scales multiplied by the accelerating electric field– giving the total energy possible if an electron was accelerated over that distance.

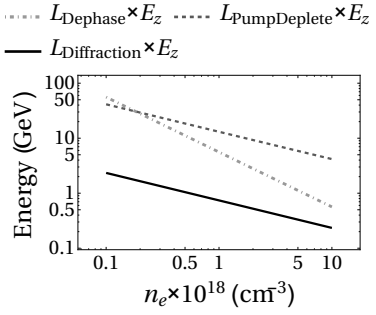

Figure 8: The three length scales involved with accelerating electrons: L_{Dephase} where the electron outruns the wave, self-limiting the total energy gained; $L_{\text{PumpDepletion}}$ where the incident energy in the laser pulse is completely transfered to the wakefield, and the laser can no longer sustain the bubble regime; and $L_{\text{Diffraction}}$ the inherent diffraction of the laser pulse. All lengths are scaled by an accelerating field using parameters from the Texas experiment[19], to show the total possible energy an electron could gain.

There are several strategies for extending the length of the laser-plasma interaction. In the following section, we will discuss the propogation of intense lasers through plasmas, and show that there are two main strategies for overcoming the inherent diffraction of the laser.

2.4 Laser Propogation in Plasma

In the previous section we discussed the limiting length scale caused by the inherent diffraction of the laser pulse. However, the plasma itself can dramatically change the propogation of the laser pulse and this can be used to overcome the diffraction limitations. To first order, we can discuss the plasma's impact on laser propogation through investigating the behaviour of the plasma's index of refraction.

The index of refraction η of a plasma is given by: $\eta c = d\omega/dk$, where ω is the frequency and k is the wavenumber of the propogating wave.

$$\eta = \left(1 - \frac{\omega_p(n_e)^2}{\omega^2}\right)^{1/2}. \tag{7}$$

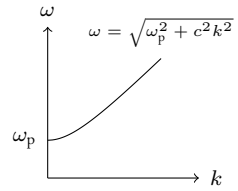

Figure 9: The plasma dispersion relation. We will be dealing with plasmas where $\omega_p/\omega << 1$, so to first order the laser will be dispersionless.

For our purposes, the most important scaling behaviour of the index of refraction is with the electrons mass and density. Recalling that ω_p scales as $\sqrt{n_e/m_e}$, η will scale as:

$$\eta = \left(1 - \frac{n_e}{m_e} f\right)^{1/2} \tag{8}$$

Recalling that a converging lens has $d\eta/dr < 0$, we can see that the plasma can counteract diffraction by acting like a converging lens in two cases: if $dn_e/dr < 0$ or $dm_e/dr > 0$. The first case is due to relativistic effects. As we discussed in Section 2.1, the first order effect of the laser is going to be accelerating them in the polarization plane: the quiver momentum. The electrons will have a maximum amount of kinetic energy as they pass through the centre of the laser pulse, and through relativity we know that this corresponds to an increase in their mass. Thus, the effective mass of the electrons will have $dm_e/dr < 0$ and the plasma will act as a focusing lens. This phenomena is refered to as relativisitic self-focusing and is used by all groups to some extent. However, in order to use relativistic self-focusing to counteract diffraction, the laser has to be intense enough to meaningfully change the mass of the electrons. This condition has been found to be $I > 17.5\,\mathrm{GW/cm^2}$[].

There are several subtlies involved with relativistic self-focusing that our proof-of-concept argument doesn't reveal. Chief amoung these is the effect of pulse length on relativistic self-focusing. If we consider that the electrons are responding to the laser at frequency ω_p, then it will take time scales on the order of $\tau_p = \frac{1}{2\pi\omega_p}$ for the relativistic effect to build up, ie. the middle of the laser pulse will be 'seeing' the relativistic index gra-

dient created by the front of the pulse. This has two main consequences: first, long pulses $\tau_{\text{duration}} > \tau_p$ are more susceptible to relativistic effects, and the front of the pulse will be constantly diffracting away. Groups that primarily use relativistic self-focusing, such as the UT Austin group, not only have to choose laser pulses that are intense enough, but also have to choose them to be long enough.

However, from Equation (8) we can see that a direct modulation of the density of the electrons can also achieve focusing effects. As long as the density goes as $dn_e/dr > 0$, we have the appropriate condition for a converging lens. This is the approach used by the UC Berkeley group, where a plasma channel is used to give the appropriate density modulation. The plasma channel is a simple tube containing hydrogen gas with a metal plate at each end. A voltage is applied across the length of the tube, ionizing the gas. The gas will cool down more rapidly along the edges of the tube, and this will give rise to an approximately parabolic density profile of the hydrogen gas[2, 16]. It is this parabolic density profile which will act as the focusing lens of the plasma wave. The evolution of a laser pulse in a plasma channel is shown in Figure 10.

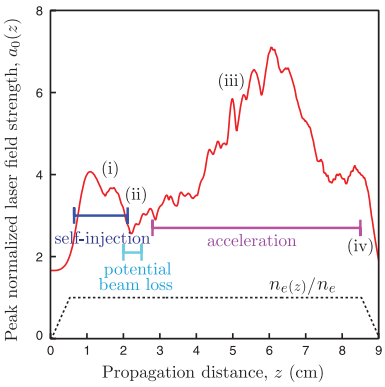

Figure 10: Evolution of the peak normalized intensity of the laser pulse, ($a_0(z)$ done using a particle-in-cell simulation for a top-hat laser pulse with energy 16 J, through a 9 cm plasma waveguide. *From Leemans et. al. 2014 [12]*

3 Experimental Set-Up and State-of-the-Art

In this review, we will focus on the experimental efforts of two groups, UT Austin Texas, and University of California Berkeley. Although there are many more groups doing interesting work in the field of LWFA, these two groups are the main ones actively pursuing the goal of high-energy electron acceleration.

The Texas group uses very high-intensity laser pulses and exploits the phenomena of relativistic self-guiding to cancel out the inherent diffraction of the laser. The Berkeley group uses low-intensity laser pulses and plasma waveguide channels to overcome the diffraction issue. A more in depth review of each group and method is presented below.

3.1 Texas

In 2013 the Texas group reported a collimated beam of 2 GeV[19].

By leveraging the new petawatt laser facility at UT Austin they were able to get firmly within the experimental constraints for relativitic self-guiding. However, due to the intense non-linear interactions involved detailed numerical work has to be done to find the right initial conditions to produce an optimal beam. One such example is shown in Figure 11[19], where by altering intial conditions such as the beam profile, startlingly different dynamics occured.

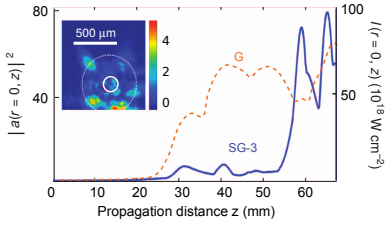

Figure 11: Simulations done by the Texas group using the WAKE code showing clear features of self-focusing.[19] As the normalized laser-intensity gets larger, the pulse is contracting–concentrating more of its energy over a smaller area. Interestingly, the self-focusing exhibits a periodic structure– going through two cycles of diffraction-focusing for the super-Gaussian pulse.

The Texas group based their experiment on a paper by[], which predicted the intial conditions needed to obtain high-quality mono-energetic beams. Although they were not able to get to the predicted energies of[], this approach was largely successful, as they were able to double the energies of previous results[18].[].

Shown in Figure 12 is the experimental setup for Texas. At its heart, it is a high-intensity laser that is hitting an ionized gas. The majority of the experiment is the diagnostics, which allow the team to determine the energy and angular spread of the electrons.

The Texas group is now hard at work trying to find a strategy to increase the energy of the electrons. As shown in Figure 11, the behaviour of the self-focusing is very dependent on initial conditions (laser intensity, laser pulse shape, etc.). As no analytic model can fully encompass its behaviour, numerical simulation is required to understand the self-focusing behaviour required to produce acceleration lengths required for high energy electrons and there are already several novel proposals to increasing the energy of the electrons[].

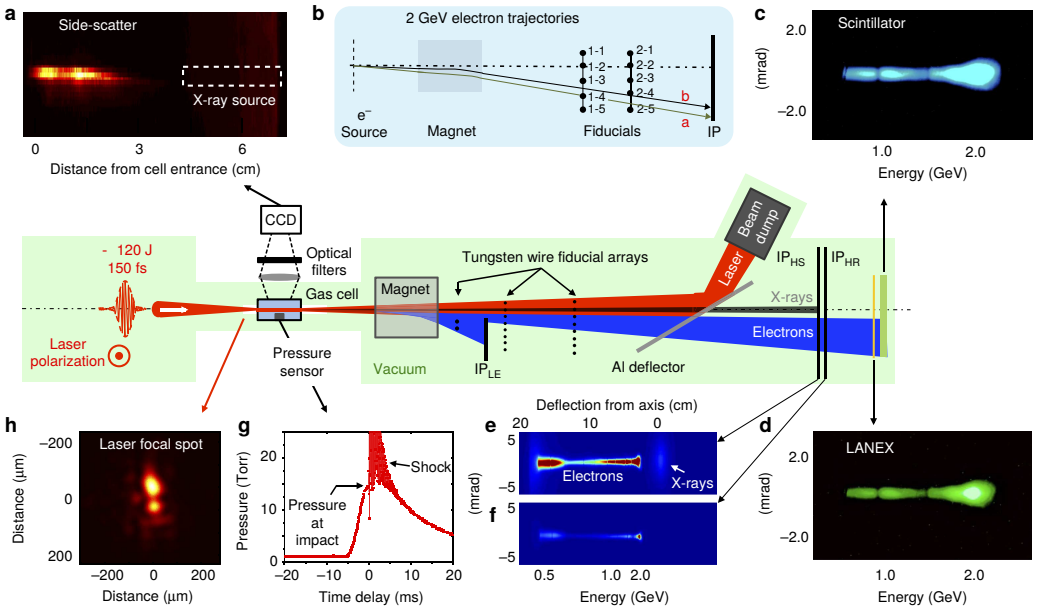

Figure 12: The experimental setup of the Texas group.[19] *This figure is reproduced from Nat. Commun. Vol. 4, 2013.* The laser hits a gas cell. It will propogate in the plasma, until the self-focusing process reaches a critical point, where the laser-plasma will enter the bubble regime. a) Detector to measure sidescatted light from gas-laser interaction. b Schematic showing how the electrons are bent using a magnet– acting like a spatial filter for momentum. There are tungsten posts that will cast 'shadows' on the electron detector, allowing the source of the electrons to be backtracked. c Electron spectrum on the scintillator. d Another spectrum on the LANEX. e)&f) X-ray beam blocker. g Pressure sensor on the gas cell. h Image of the laser spot-size.

3.2 UC Berkeley

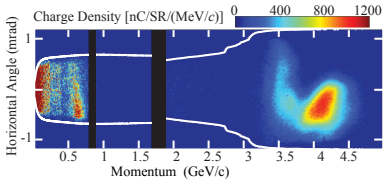

Figure 13: The energy spectrum for the recent Berkeley result.

In 2014, the Berkeley group reported a collimated electron beam with peak energy of 4.2 GeV. They achieved this through a slightly different experimental philosophy than the Texas group. By using lower-intensity short-duration lasers, they are able to use a plasma-channel guide. Although relativistic self-focusing is still required to achieve the high-intensities needed for the bubble regime, the plasma-channel does the majority of the work in preventing laser diffraction. Their use of a lower intensity laser has two main benefits. First, they signifigantly gain on energy conversion efficiency, although the acceleration gradients are smaller, they are able to guide them over larger distances. Second, because the laser is lower intensity, the dynamics of relativistic self-focusing and non-linear laser-plasma interactions are less pronounced, greatly simplifying the dynamics of the laser propogation. However, they will ultimately be limited by the pump-depletion length, as the laser simply has less energy than the Texas petawatt laser.

4 Conclusion

In this review, we have highlighted two approaches for electron acceleration: the high-intensity, relativistically guiding approach used by Texas, and the low-intensity, plasma-channel guided approached used by Berkeley. For further progress to be made in the field, there needs to be a better understanding of the evolution of the laser-plasma interaction and evolution. It is worth noting that the bubble regime– the regime used by all groups trying to achieve GeV acceleration– was first seen in simulations.

New imaging techniques at UT Texas, which allow in vivo imaging of the evolution of the laser and plasmon, as well as novel theoretical and computational approaches are the current frontier. The raw power exists to accelerate electrons to high GeV energies, all we need to do is control it.

References

[1] Sterling Backus, Charles G Durfee III, Margaret M Murnane, and Henry C Kapteyn. High power ultrafast lasers. *Review of scientific instruments*, 69(3):1207–1223, 1998.

[2] A. Butler, D. J. Spence, and S. M. Hooker. Guiding of high-intensity laser pulses with a hydrogen-filled capillary discharge waveguide. *Phys. Rev. Lett.*, 89:185003, Oct 2002.

[3] The ATLAS Collaboration. A particle consistent with the higgs boson observed with the atlas detector at the large hadron collider. *Science*, 338(6114):1576–1582, 2012.

[4] C. D. Decker, W. B. Mori, K.-C. Tzeng, and T. Katsouleas. The evolution of ultra-intense, short-pulse lasers in underdense plasmas. *Physics of Plasmas (1994-present)*, 3(5), 1996.

[5] E. Esarey, C. B. Schroeder, and W. P. Leemans. Physics of laser-driven plasma-based electron accelerators. *Rev. Mod. Phys.*, 81:1229–1285, Aug 2009.

[6] Eric Esarey and Mark Pilloff. Trapping and acceleration in nonlinear plasma waves. *Physics of Plasmas (1994-present)*, 2(5), 1995.

[7] Jérôme Faure, Yannick Glinec, A Pukhov, S Kiselev, S Gordienko, E Lefebvre, J-P Rousseau, F Burgy, and Victor Malka. A laser–plasma accelerator producing monoenergetic electron beams. *Nature*, 431(7008):541–544, 2004.

[8] C. G. R. Geddes, Cs Toth, J. van Tilborg, E. Esarey, C. B. Schroeder, D. Bruhwiler, C. Nieter, J. Cary, and W. P. Leemans. High-quality electron beams from a laser wakefield accelerator using plasma-channel guiding. *Nature*, 431(7008):538–541, Sep 2004.

[9] Guillaume Genoud. *Laser-Driven Plasma Waves for Particle Acceleration and X-Ray Production*. PhD thesis, Lund University, 2011.

[10] LM Gorbunov and VI Kirsanov. Excitation of plasma waves by an electromagnetic wave packet. *Sov. Phys. JETP*, 66(290-294):40, 1987.

[11] I. Kostyukov, E. Nerush, A. Pukhov, and V. Seredov. Electron self-injection in multidimensional relativistic-plasma wake fields. *Phys. Rev. Lett.*, 103:175003, Oct 2009.

[12] P. Leemans, W. J. Gonsalves, A. H.-S. Mao, K. Nakamura, C. Benedetti, B. Schroeder, C. Cs. Tóth, J. Daniels, E. Mittelberger, D. S. Bulanov, S. J.-L. Vay, C. G. R. Geddes, and E. Esarey. Multi-gev electron beams from capillary-discharge-guided subpetawatt laser pulses in the self-trapping regime. *Phys. Rev. Lett.*, 113:245002, Dec 2014.

[13] W. P. Leemans, B. Nagler, A. J. Gonsalves, Cs Toth, K. Nakamura, C. G. R. Geddes, E. Esarey, C. B. Schroeder, and S. M. Hooker. Gev electron beams from a centimetre-scale accelerator. *Nat Phys*, 2(10):696–699, Oct 2006.

[14] SPD Mangles, CD Murphy, Z Najmudin, AGR Thomas, JL Collier, AE Dangor, EJ Divall, PS Foster, JG Gallacher, CJ Hooker, et al. Monoenergetic beams of relativistic electrons from intense laser–plasma interactions. *Nature*, 431(7008):535–538, 2004.

[15] Patrick G O'Shea and Henry P Freund. Free-electron lasers: status and applications. *Science*, 292(5523):1853–1858, 2001.

[16] D. J. Spence and S. M. Hooker. Investigation of a hydrogen plasma waveguide. *Phys. Rev. E*, 63:015401, Dec 2000.

[17] T. Tajima and J. M. Dawson. Laser electron accelerator. *Phys. Rev. Lett.*, 43:267–270, Jul 1979.

[18] M. Tzoufras, S. Tsung, F. B. Mori, W. and A. Sahai, A. Improving the self-guiding of an ultraintense laser by tailoring its longitudinal profile. *Phys. Rev. Lett.*, 113:245001, Dec 2014.

[19] Xiaoming Wang, Rafal Zgadzaj, Neil Fazel, Zhengyan Li, S. A. Yi, Xi Zhang, Watson Henderson, Y.-Y. Chang, R. Korzekwa, H.-E. Tsai, C.-H. Pai, H. Quevedo, G. Dyer, E. Gaul, M. Martinez, A. C. Bernstein, T. Borger, M. Spinks, M. Donovan, V. Khudik, G. Shvets, T. Ditmire, and M. C. Downer. Quasi-monoenergetic laser-plasma acceleration of electrons to 2 gev. *Nat Commun*, 4, Jun 2013. Article.